



## Stability Improvement of Humic Acid as Sorbent through Magnetite and Chitin Modification

Bambang Rusdiarso<sup>a,\*</sup>, Rahmat Basuki<sup>a</sup>

<sup>a</sup> Department of Chemistry, Faculty of Mathematics and Natural Sciences, Universitas Gadjah Mada, Yogyakarta, Indonesia

\*Corresponding author: 1. [brusdi\\_mipa@ugm.ac.id](mailto:brusdi_mipa@ugm.ac.id)\*

<https://doi.org/10.14710/jksa.23.5.152-159>



### Article Info

#### Article history:

Received: 31<sup>st</sup> December 2019

Revised: 20<sup>th</sup> April 2020

Accepted: 2<sup>nd</sup> May 2020

Online: 31<sup>st</sup> May 2020

#### Keywords:

HA stabilization; HA modification; magnetite/HA-chitin; Hg(II)

### Abstract

Stability improvement of humic acid (HA) through modification of HA by chitin (HA-chitin) followed by a coating of HA-chitin on magnetite has been successfully performed. The coated magnetite (magnetite/HA-chitin) was conducted by the co-precipitation method, and the synthesized magnetite/HA-chitin was characterized by FT-IR, XRD, SEM-EDX, and VSM. The successful coated-magnetite by HA-chitin was proved by the appearance of a new band at 1627 cm<sup>-1</sup> (FT-IR), the formation of a crystalline phase with characteristic  $2\theta$  of magnetite: 30.259° [220]; 35.64° [311]; 42.590° [400]; 57.280° [511]; and 62.896° [440] (XRD), an increasing of carbon content in magnetite/HA-chitin (SEM-EDX), and the ease of magnetite/HA-chitin being attracted to external magnetic fields with magnetic saturation strength 29.3 emu/g (VSM). Stability tests at pH 2.0 - 10.0 prove that magnetite/HA-chitin remains stable as a solid sorbent on average above 80%. Its application to Hg (II) sorption occurred optimum at pH 7.0, where 75.89% Hg (II) is sorbed on 0.1 g of sorbent and agreed well to the pseudo-second-order kinetics model of Ho.

### 1. Introduction

Humic acid (HA) is a macromolecular compound of functional groups that is stable at the acidic condition. HA (humus) is the end of lignin decomposition, which is abundantly found in peat soils [1]. HA has been reported to possibly interact with more than 50 chemical compounds ranging from heavy metals, organic compounds, and radioactive [2]. HA is an excellent sorbent for heavy metals because of its high capacity and sorption rate [3]. In the perspective of environmental management, this excellence makes HA widely developed because of its high affinity with metal cations. Compared to activated carbon [4, 5], bentonite [5, 6], and metal oxides [7, 8], HA shows a higher capacity and sorption rate than those materials [9].

The weakness of HA as a solid material is its stability, which only occurs at pH < 2.0. At pH > 2.0, HA slowly starts to dissolve due to deprotonation in HA function groups which is dominated by carboxylates and phenolics to a maximum of pH=5.0, and 90% HA is dissolved at pH 7.0 [10]. Consider its low stability at pH > 5.0; several studies have been performed to improve the stability of HA through several modification techniques. Chitin

immobilized to HA has been shown to enhance the stability of HA as a solid sorbent up to pH=12.0 [11]. Besides, chitin also provides additional nitrogen groups as potential active sites for binding metal cations. However, the application of HA-Chitin still requires impractical filtration steps after the sorption process.

This study aims to improve the stability of HA by modifying it with chitin. Then the HA-chitin is coated onto magnetite to obtain easy handling separation after the sorption process by an external magnet. The resulting sorbent material (magnetite/HA-chitin) was then characterized by Fourier Transform-Infra Red Spectrophotometer (FT-IR), Scanning Electron Microscopy-Energy Dispersive X-ray (SEM-EDX), X-Ray diffractometer (XRD), and vibrating sample magnetization (VSM). Magnetite/HA-chitin was also applied to remove harmful heavy metal cations of Hg(II) in the solution. Furthermore, the characterization of magnetite/HA-chitin and previous composer (HA, chitin, and magnetite) and the sorption parameters of Hg(II) will also be profoundly discussed in this paper.

## 2. Methodology

### 2.1. Materials

All reagent used in this work was analytical grades (pro-analyst) provided by E. Merck, i.e., NaOH pellets, concentrated HCl,  $\text{FeCl}_3 \cdot 6\text{H}_2\text{O}$  powder,  $\text{FeSO}_4 \cdot 7\text{H}_2\text{O}$  powder, concentrated HF and  $\text{HgCl}_2$  as a source of Hg(II). Peat soil as a source of HA was taken from the Londerang Forest, Jambi, Indonesia. Chitin was isolated from the waste shrimp shell of a seafood restaurant in Yogyakarta, Indonesia.

### 2.2. Instrumentation

Instrumental analysis of functional group was performed by Shimadzu Prestige 21 (FT-IR); morphology and elemental analysis by JSM-6510LA (SEM-EDX); crystal analysis by Rigaku Miniflex600 with Cu light 40 kW 15 mA (XRD), and magnetic characterization by OXFORD VSM 1,2H (VSM).

### 2.3. Extraction and purification of HA

HA extraction was conducted based on IHSS (International Humic Substance Society) recommendations [12] through 200 mesh 100 g of dry peat soil powder was acidified to pH=1.0 using 4 M HCl. After 24 hours, the mixture was separated to take the residue. The solid residual was mixed with 1 L NaOH 1 M and stirred for 24 hours. The suspension was centrifuged at 5000 rpm for 15 minutes to separate HA (solid) and fulvic acid, FA (filtrate). The HA resulted from centrifugation was then dried at 60°C. Purification of HA was carried out with HCl/HF (1:3) method to remove silica minerals. FT-IR then characterized the purified HA.

### 2.4. Isolation of chitin

Chitin isolation was performed according to No *et al.* [13] method, which consists of deproteination and demineralization steps. Deproteination was conducted through refluxing 25 g of shrimp shell powder in 250 mL NaOH 3.5% (w/v) at 65°C for 2 hours. The result was cooled, and then the residue was filtered. The residue was washed with distilled water to a neutral pH and then dried at 60°C. Protein-free shrimp's shell was reacted with 1 M HCl at a ratio of 1:15 (w/v) and stirred for 30 minutes at room temperature, then filtered and washed with distilled water to neutral pH. Isolated chitin was characterized by FTIR and shrimp shell as chitin's raw material was characterized by SEM-EDX.

### 2.5. Immobilization HA on chitin (HA-Chitin)

Forty grams of chitin were put into 250 mL of 0.5 M HCl to form a very thick solution (activated chitin). Chitin activated afterward was reacted with 4 g HA in 500 mL NaOH 0.5 M. The reaction was run for 24 hours while stirring, the formed solids were separated, filtered, and dried at 40°C to a constant weight. FTIR, SEM-EDX, and XRD characterized the formed HA-Chitin.

### 2.6. HA-chitin magnetization

HA-chitin magnetization was synthesized using the co-precipitation method [14]. 1.525 g  $\text{FeCl}_3 \cdot 6\text{H}_2\text{O}$  and 1.05 g  $\text{FeSO}_4 \cdot 7\text{H}_2\text{O}$  were dissolved in 25 mL of distilled water

and heated to 90°C. 10 mL of 25%  $\text{NH}_4\text{OH}$  was added together with a mixture of 0.25 g HA-chitin in 1 M NaOH and 12.5 mL of distilled water for 24 hours. The mixture was stirred at 90°C for 30 minutes and cooled to room temperature. The black precipitate was then separated from the solution and washed to neutral using distilled water. HA-chitin magnetic characterization was carried out using FTIR, XRD, SEM-EDX, and VSM.

### 2.7. Sorbent Stability test in various medium acidity

A total of 50 mg of sample was put into a solution with a pH of 2.0 to 10.0, then stirred for 2 hours then left for 24 hours until everything in the sorbent dissolved. The content of humic acid released into the solution was determined by weighing the remaining insoluble solids.

### 2.8. Optimum pH of Hg (II) sorption

A total of 0.1 g of the sample interacted separately with each 50 mL 100 mg/L metal ion solution which varied at pH 3.0; 4.0; 5.0; 6.0 and 7.0 then stir for 120 minutes. The mixture was then filtered, and the filtrate was taken. Metal ion concentrations before and after sorption were analyzed by Mercury Analyzer (Lab Analyzer 254). The optimum pH of sorption was determined by looking at the highest amount of adsorbate sorbed.

### 2.9. Sorption kinetics

A total of 0.1 g of the sample has interacted with 50 mL of 380 mg/L metal ion solution at optimum pH. This mixture was then stirred with time variations of 15, 30, 60, 90, and 120 minutes. After reaching the specified time limit, each suspension was filtered, and the filtrate was taken. Hg (II) concentrations before and after sorption were analyzed by Mercury Analyzer.

## 3. Results and Discussion

### 3.1. Characterization of Magnetite/HA-Chitin

FT-IR spectroscopy has been used for analysis HA, chitin, HA-chitin, magnetite, and magnetite/HA-chitin functional groups from synthesis (Figure 1). HA and HA-chitin provide sharp band absorption at  $1710\text{ cm}^{-1}$ , which indicates the carboxylic group. However, only HA, chitin, and HA-chitin provide absorption at approximately  $1419\text{ cm}^{-1}$ , which is specifically associated with the bending of a C-O-H carboxylic group. The carboxylate levels determined using the  $I_{\text{Ar}}/I_{\text{COOH}}$  ratio (ratio of intensity at  $1510\text{ cm}^{-1}$  to the intensity at  $1419\text{ cm}^{-1}$ ) show that chitin has the most significant ratio (Table 1). However, compared to chitin, HA has the highest  $I_{\text{Ar}}$  and  $I_{\text{COOH}}$  values, although it produces  $I_{\text{Ar}}/I_{\text{COOH}}$  ratio that is slightly smaller than chitin [15].

Another significant absorption band is at  $1627\text{ cm}^{-1}$  caused by stretching the aromatic C=C group or stretching C=O from the conjugated hydrogen ketone and quinone bonds. This absorption appears with high intensity for HA and chitin but does not appear in magnetite. Another aromatic absorption is seen at  $1510\text{ cm}^{-1}$  caused by stretching C=C aromatic lignin residues whose intensity is minimal, even in HA. Low lignin residues indicate that lignin has transformed into HA. This claim is supported by  $I_{\text{Ar}}/I_{\text{Al}}$  ratio data (ratio of intensity at  $1510\text{ cm}^{-1}$  to the

intensity at 2924 cm<sup>-1</sup>) used to estimate aromaticity. The I<sub>Ar</sub>/I<sub>Al</sub> ratio (Table 1) shows that HA aromaticity is highest compared to other materials. Absorption of broadband centered around 3448 cm<sup>-1</sup> indicates the O-H stretching of various functional groups connected by hydrogen bonds between molecules. The appearance of the aliphatic chain is observed at 3000–2800 cm<sup>-1</sup>. The presence of aliphatic groups is expressed by the band at 2924 cm<sup>-1</sup>, which is associated with the asymmetric C-H strains of the methylene group [15]. The band around 2850 cm<sup>-1</sup> is related to the C-H strain of the group -CH<sub>2</sub>- which also appears as a deformation band at 1072 cm<sup>-1</sup> [15, 16].

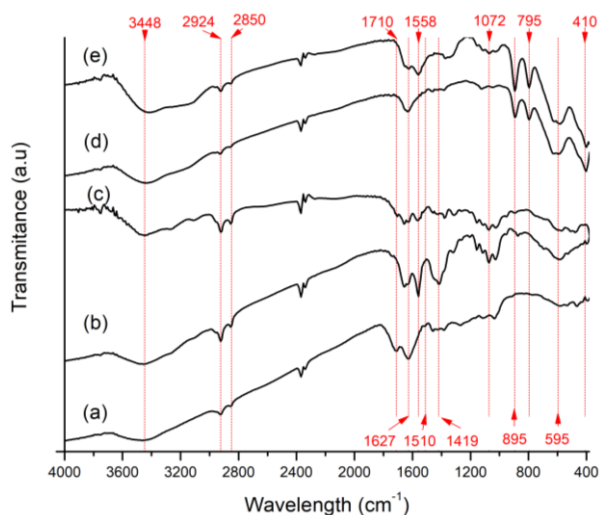


**Figure 1.** FT-IR spectra of (a) HA, (b) chitin, (c) HA-Chitin, (d) Magnetite, and (e) Magnetite/HA-chitin

**Table 1.** The ratio of carboxylate (I<sub>Ar</sub>/I<sub>COOH</sub>) and aromaticity (I<sub>Ar</sub>/I<sub>Al</sub>) degree of the synthesized material

Materials	I <sub>Ar</sub> (1510 cm <sup>-1</sup> )	I <sub>COOH</sub> (1419 cm <sup>-1</sup> )	I <sub>Al</sub> (2924 cm <sup>-1</sup> )	I <sub>Ar</sub> /I <sub>COOH</sub>	I <sub>Ar</sub> /I <sub>Al</sub>
HA	33.94	33.13	12.53	1.02	2.71
chitin	31.98	26.31	12.52	1.22	2.55
HA-chitin	36.22	35.21	30.81	1.03	1.18
Magnetite	28.57	29.14	13.67	0.98	2.09
Magnetite/HA-chitin	23.88	25.70	16.63	0.93	1.44

The all sharp and intensive HA, HA-chitin, and magnetite/HA-chitin spectra at 1558 cm<sup>-1</sup> indicate a secondary amide group. Some authors consider the band at around 1660 cm<sup>-1</sup> to be an indicator of a protein-like substance [17]. The main difference between HA and chitin spectrum is the appearance of absorption in 1419 and 1558 cm<sup>-1</sup>. The first region is characterized by a sharp band at 1419 cm<sup>-1</sup> which indicates aromatic skeletal vibration combined with CH in-plane deformation for cellulose-like compound [18] and a relatively intense band at 1558 cm<sup>-1</sup>, which is a stretching vibration of N-H

in amides [17]. Compared with chitin, HA has not shown spectra at 1419 and 1558 cm<sup>-1</sup>. Widened peaks at wavelengths less than 650 cm<sup>-1</sup> are associated with minerals such as kaolinite, silica and other minerals.

The successful coating of HA-chitin on magnetite is shown by the constant absorption at 895 and 795 cm<sup>-1</sup> on magnetite/HA-chitin (Figures 1(d) and 1(e)) which are typical Fe-O absorption of magnetite [16, 17, 18, 19]. The IR spectra shows the C=O strain of magnetite/HA-chitin at ~ 1627 cm<sup>-1</sup>, which shows the interaction of carboxylic anions with FeO surfaces, such as C=O free from carboxylic acids above 1700 cm<sup>-1</sup>, where this absorption is not found in magnetite spectra which indicates bonding occurs due to ligand exchange. UV-vis analysis of Illés and Tombácz [20] showed a redshift reinforces the alleged binding of HA to the surface of Fe<sub>3</sub>O<sub>4</sub> by ligand exchange. Similar results were revealed by Zarghani and Akhlaghinia [21] that the -COO group is a group that plays an essential role in the complexation of metal cations. FT-IR revealed that the -COO- and N-acetyl groups are groups involved in the sorption of Cr(III) in the sorbent HA-chitin (HA-chitin) immobilized. Before, the sorption of HA-chitin showed a typical absorption of chitin at 1419 cm<sup>-1</sup>, which is symmetrical and asymmetric bend of C-CH<sub>3</sub>; and 1558 cm<sup>-1</sup>, which is a characteristic of the N-C strain (Figure 1(b)). The disappearing of the absorption peak, indicating the reaction between HA and metal in the replacement of C=O, was observed at 1710 cm<sup>-1</sup>.

Analysis of magnetite/HA-chitin crystallinity using XRD shows that magnetite/HA-chitin is crystalline with 2θ characteristics for magnetite at 30.259° [220]; 35.64° [311]; 42.590° [400]; 57.280° [511]; and 62.896° [440] (Figure 2b) [22, 23]. The XRD peak corresponds to the characteristic peak of the inverted cubic spinel structure (JCPDS 65-3107) [24]. These results indicate that the crystalline structure of Fe<sub>3</sub>O<sub>4</sub> did not change after being modified using HA-chitin. HA-chitin coating on the surface of Fe<sub>3</sub>O<sub>4</sub> relatively increases the intensity of the diffractogram peaks, which indicates that the coating of HA-chitin increases the crystallinity and stability of the magnetite [25]. The opposite results from the decrease in 2θ peak intensity were also reported by Krisbiantoro *et al.* [24], who coated magnetites with fulvic acid and humic acid [26]. These results suggest that the presence of chitin in AH can improve the crystallinity of magnetite in magnetite/AH-chitin.

The magnetite and magnetite/HA-chitin saturation were measured at 37.6 and 29.3 emu/g, respectively (Figure 2a). Separation of magnetite/HA-chitin from the dispersion of the solution can be conducted using an external magnet in a relatively short time. A simple qualitative test for the magnetic properties of magnetite/HA-chitin was performed by an external magnetic field attraction test. Figure 5(a) shows the dispersion of magnetite/HA-chitin being attracted by an external magnet and then dispersed again in solution after the magnetic field disappears.

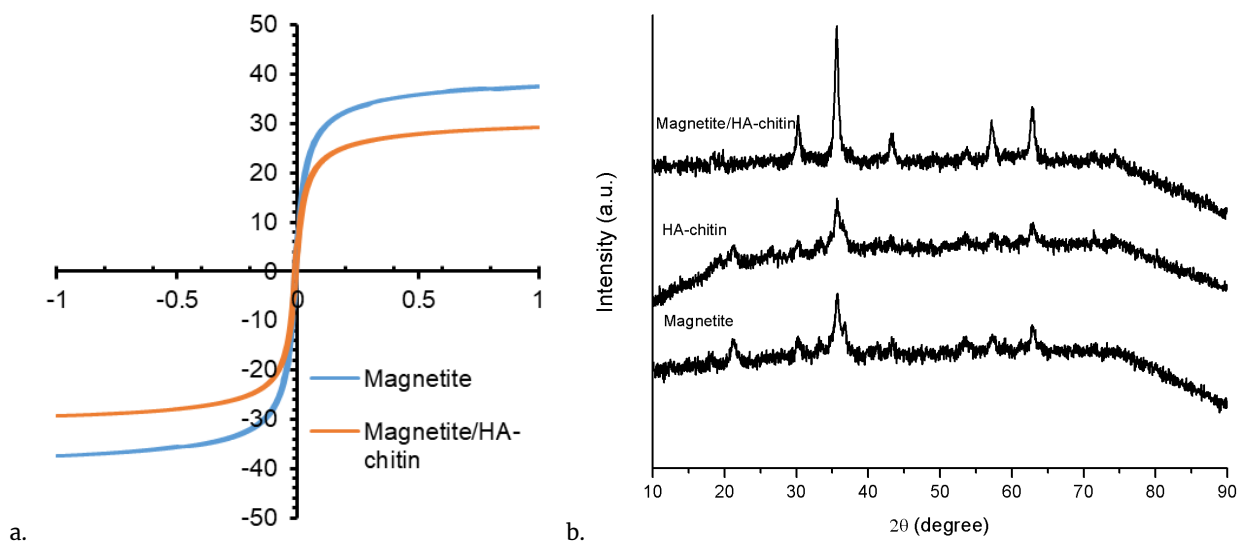


Figure 2. (a) Magnetization saturation analysis of magnetite and magnetite/HA-chitin; and (b) Diffractogram of magnetite/HA-chitin, HA-chitin, and magnetite

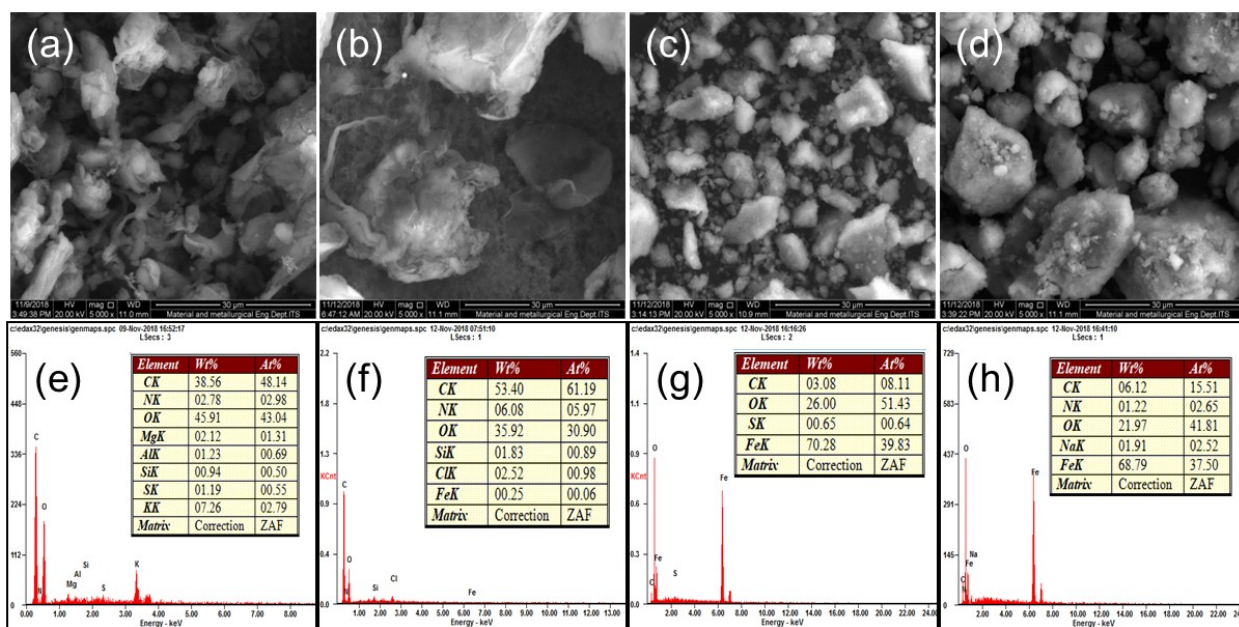


Figure 3. Morphological analysis by SEM (a-d) 5000 × magnification and elemental analysis by EDX (e-h) of shrimp shells (a and e); HA-chitin (b and f); Magnetite (c and g); and Magnetite/HA-chitin (d and h).

The attraction of magnetite/HA-chitin to an external magnetic field shows that AH coating on the magnetite surface reduces the magnetic strength of the magnetite but is still relatively strong enough to be attracted by the external magnetic field in a short time, less than 2 minutes [27]. The black suspension of pure magnetite can be easily oxidized to a brown suspension without magnetization. Peng *et al.* [28] reported that the synthesized magnetite/HA-chitin did not experience significant color changes and magnetization saturation after being stored in distilled water for one month. These results indicate that AH coating on magnetite can prevent oxidation and maintain the saturation value of magnetization.

The morphological appearance of shrimp shells and HA-chitin are irregularly shaped with obtuse and webbed angles with sizes of 10–20 μm (Figures 3a and 3b). While magnetite is almost the same size, it has a fractal shape

with sharp angles and agglomerates (Figure 3d). HA-chitin coating on magnetite appears to increase the size of magnetite particles so that magnetite/HA-chitin tends to be larger than magnetite because of the successful coating of HA-chitin on the surface of the magnetite [29]. EDX analysis showed that HA-chitin (Figure 3f) is dominated by elements C (53.40%), O (35.92%), and a small amount of iron, Fe (0.25%). Meanwhile, magnetite (Figure 3g) is dominated by Fe (70.28%), O (26.00%), and a small amount of C (3.08%). The HA coating on magnetite is observed to reduce the composition of Fe magnetite to 68.79% and increase carbon and oxygen to 6.12% and 21.97% respectively (Figure 3h). This evidence confirms that the coating of AH-chitin on magnetite was successfully performed.

### 3.2. Effect of pH on Stability and sorption of Hg (II) onto Magnetite/HA-chitin

The HA coating on the magnetite surface can increase the stability of Fe and HA ions (Figure 4a). Magnetite is less stable at low pH because Fe<sup>2+</sup> ions from magnetite will be released and oxidized to form γ-Fe<sub>2</sub>O<sub>3</sub>, which has smaller magnetic properties [25, 26] whereas HA is less stable at high pH (above 5.0) due to deprotonation of the -OH phenolate and -COOH functional groups. The HA coating on magnetite improves stability so that magnetite/HA-chitin is stable at both low and high pH [20]. Figure 4(a) shows that magnetite/HA-chitin shows relatively high stability as a solid in the pH range 2.0 - 10.0. There is an anomaly at pH 4.0 - 6.0 where the stability decreases, which is presumed because both the magnetite material and HA-chitin are at stability that is equally weak and does not reinforce each other.

The effect of pH on the sorption of Hg(II) by magnetite/HA-chitin is shown in Figure 4(b). The absorption of Hg (II) on magnetite/HA-chitin is significantly affected by the pH at which optimal sorption occurs at pH 7.0. This shows that the change in pH of the solution results in a magnetic surface charge that is different from magnetite/HA-chitin. When the pH is relatively high, the surface of the magnetite/HA-chitin has a negative charge due to the deprotonation of the carboxylic and phenolate HA functional groups and causes strong interactions with the Hg(II) ions [30]. If the pH condition is deficient, the protonation of the magnetite/HA-chitin magnetic function group is very strong so that the sorbent surface is positively charged and a repulsion occurs between the magnetite/HA-chitin functional group with Hg(II) which causes a decrease in the absorption of Hg(II) at acidic pH.

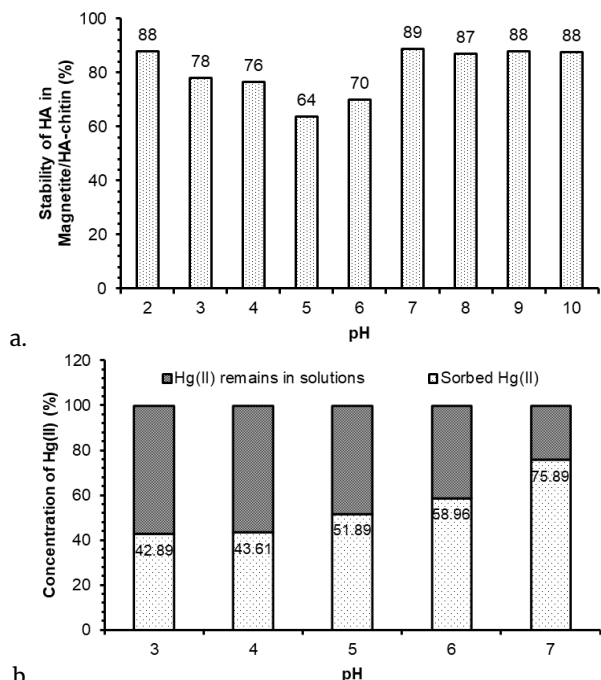


Figure 4. (a) Magnetite/HA-chitin stability at pH 2.0 - 10.0; (b) Effects of pH on sorption of Hg (II) on magnetite/HA-chitin (50 mL Hg(II) 100 mg/L; 0.1 g sorbent)

### 3.3. Hg(II) sorption kinetics on magnetite/HA-chitin

The absorption of Hg(II) on magnetite/HA-chitin occurs rapidly in the first 40 minutes then slows down until the sorbed Hg(II) reaches equilibrium after 120 minutes (Figure 5b). Lagergren pseudo-first-order kinetics model and Ho pseudo-second-order model were used to analyze the Hg(II) sorption kinetics on magnetite/HA-chitin. The Lagergren pseudo-first-order model can be written as [31]:

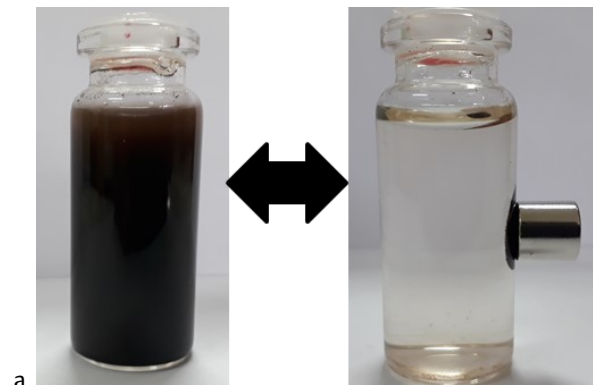
$$\log(q_e - q_t) = \log(q_e) - k_{Lag}t \tag{1}$$

Where  $q_e$  and  $q_t$  are the amounts of Hg(II) sorbed at equilibrium at time  $t$  per gram of sorbent (mg/g), and  $k_{Lag}$  is the rate constant of the Lagergren reaction (min<sup>-1</sup>). The theoretical  $k_{Lag}$  and  $q_e$  values are determined from the plot  $\log(q_e - q_t)$  vs.  $t$  by calculating the slope and intercept values of the linear regression equation (1) (Figure 5c).

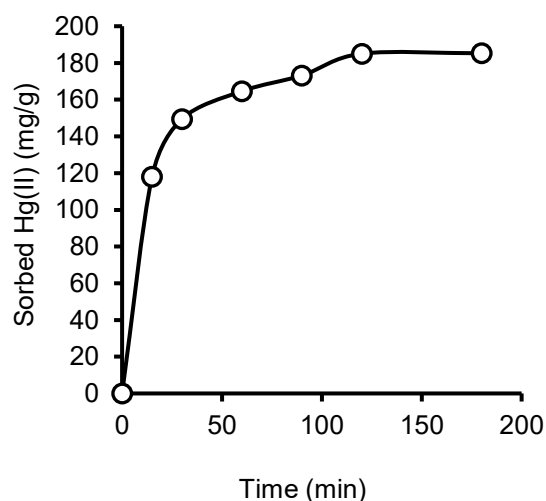
The pseudo-second-order kinetics model of Ho is written as [32]:

$$\frac{t}{q_t} = \frac{1}{k_{Ho}q_e^2} + \frac{1}{q_e}t \tag{2}$$

Where  $q_e$  and  $q_t$  are the amounts of Hg(II) sorbed at equilibrium at time  $t$  per gram of sorbent (mg/g), and  $k_{Ho}$  is the rate reaction rate of Ho (g mg<sup>-1</sup> min<sup>-1</sup>). The theoretical  $k_{Ho}$  and  $q_e$  values are determined from the plot of  $t/q_t$  vs.  $t$  by calculating the slope and intercept values of the linear regression equation (2) (Figure 5d). The kinetic parameters of the linear relationship of the Lagergren and Ho plots are tabulated in Table 2.



a.



b.

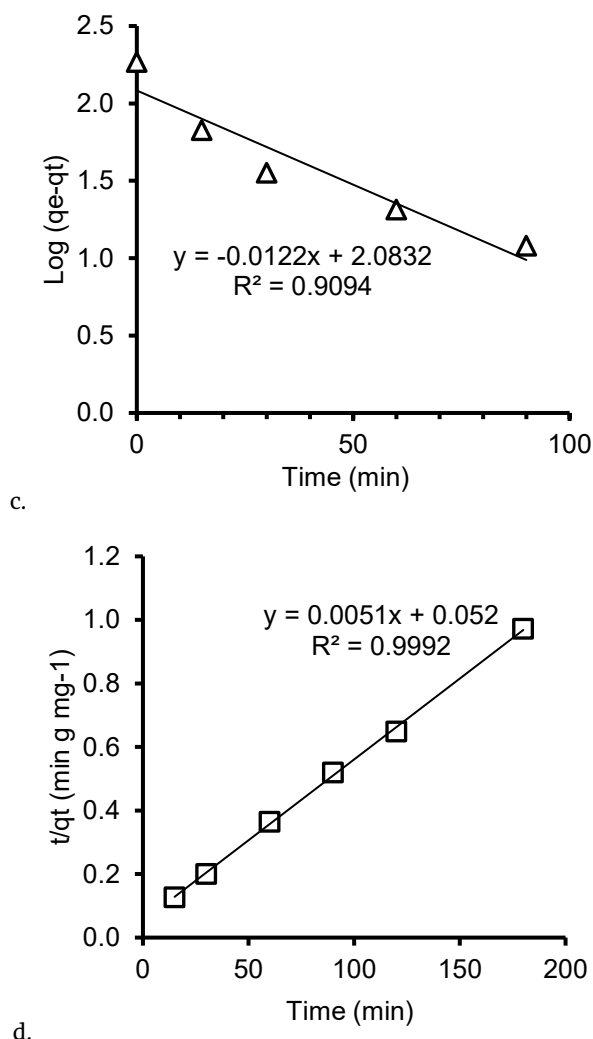


**Figure 5.** (a) Qualitative test of the magnetite/HA-chitin magnetic properties attracted by the external magnetic field; (b) Hg(II) sorption profile on magnetite/HA-chitin as a function of time; (c) Plot model of Lagergren pseudo-first order adsorption; and (d) Ho pseudo-second order Hg(II) on magnetite/HA-chitin (sorbent weight 0.1 g; 50 mL Hg(II) 380 mg/L; pH 7.0; RTP).

**Table 2.** Kinetics parameters of Lagergren pseudo-first-order plot and Ho second-order sorption of 50 mL Hg(II) 380 mg/L at 0.1 g magnetite/HA-chitin

Lagergren pseudo-first-order	$q_e$ (mg/g)	121.12
	$k_{Lag}$ ( $\times 10^{-4}$ min $^{-1}$ )	280.97
	$R^2$	0.9094
Ho pseudo-second-order	$q_e$ (mg/g)	196.08
	$k_{Ho}$ ( $\times 10^{-4}$ g mg $^{-1}$ min $^{-1}$ )	5.00
	$R^2$	0.9992

Linearity ( $R^2$ ) of the Ho second-order model is better agreed well than the Lagergren pseudo-first-order (Table 2). This condition indicates there is no significant difference between the amount of Hg(II) and the active site on the surface of magnetite/HA-chitin. However, because the  $R^2$  of the Lagergren pseudo-first-order is quite high, the system can approve more Hg(II) than the active site on the magnetite/HA-chitin surface. The theoretical  $q_e$  value of the Ho second-order model, which is closer to the experimental  $q_e$  value (185.25 mg/g), confirms that the kinetics sorption of Hg(II) on magnetite/HA-chitin follows the Ho second-order model. Similar results were also reported, among others, by Wang *et al.* [33] who conducted a study of Hg (II) sorption kinetics on magnetic  $Fe_3O_4@SiO_2-SH$  nanoparticles; Rezgui *et al.* [34] who conducted a study of Hg(II) sorption on lignocellulose; and Caner *et al.* [35] who conducted a study of Hg(II) sorption on chitosan-coated diatoms.

#### 4. Conclusion

The coating of AH-chitin on the surface of magnetite has been shown to increase magnetite stability under various acidity conditions and prevent oxidation from magnetite. The successful coating of AH-chitin on magnetite is proven by functional group analysis using FT-IR (appearance of spectra at  $1627\text{ cm}^{-1}$  on magnetite/HA-chitin), crystallinity analysis using XRD (crystalline phase of magnetite/AH-chitin with  $2\theta$  typical magnetite on  $30,259^\circ$  [220];  $35,64^\circ$  [311];  $42,590^\circ$  [400];  $57,280^\circ$  [511] and  $62,896^\circ$  [440]), SEM-EDX analysis (an increase in carbon content in magnetite/HA-chitin), and VSM analysis (magnetite/HA-chitin has a magnetic saturation strength of 29.3 emu/g). Stability tests in the range of pH 2.0 - 10.0 prove that magnetite/HA-chitin remains stable as an adsorbent solid on average above 80%. Application of magnetite/HA-chitin to Hg(II) sorption was optimum at pH 7.0, where 75.89% Hg(II) was sorbed at 0.1 g sorbent and followed the Ho pseudo-second-order kinetics model.

#### Acknowledgment

The author thanks to the Ministry of Research and Technology of Higher Education for partially support the funding for this research through the WCP program, Contract Number: 123.19/D2.3/KP/2018, and LPDP BPI Establishment Number: KET-3/LPDP.3/2018.

#### References

- [1] Mansi Rastogi, Meenakshi Nandal and Lata Nain, Additive effect of cow dung slurry and cellulolytic bacterial inoculation on humic fractions during composting of municipal solid waste, *International Journal of Recycling of Organic Waste in Agriculture*, 8, 3, (2019), 325-332 <https://doi.org/10.1007/s40093-019-0277-3>
- [2] N. S. Barot and H. K. Bagla, Extraction of humic acid from biological matrix – dry cow dung powder, *Green Chemistry Letters and Reviews*, 2, 4, (2009), 217-221 <https://doi.org/10.1080/17518250903334290>
- [3] NB Singh, Garima Nagpal and Sonal Agrawal, Water purification by using adsorbents: a review,

- Environmental technology & innovation*, 11, (2018), 187–240 <https://doi.org/10.1016/j.eti.2018.05.006>
- [4] Arnelli Arnelli, Ulya Hanifah Henrika Putri, Fandi Nasrun Cholis and Yayuk Astuti, Use of Microwave Radiation for Activating Carbon from Rice Husk Using  $ZnCl_2$  Activator, *Jurnal Kimia Sains dan Aplikasi*, 22, 6, (2019), 282–291 <https://doi.org/10.14710/jksa.22.6.282-291>
- [5] Aseel M Aljeboree, Abbas N Alshirifi and Ayad F Alkaim, Kinetics and equilibrium study for the adsorption of textile dyes on coconut shell activated carbon, *Arabian journal of chemistry*, 10, (2017), S3381–S3393 <https://doi.org/10.1016/j.arabjc.2014.01.020>
- [6] Wei Mo, Qiuzhi He, Xiujian Su, Shaojian Ma, Jinpeng Feng and Zhenli He, Preparation and characterization of a granular bentonite composite adsorbent and its application for  $Pb^{2+}$  adsorption, *Applied Clay Science*, 159, (2018), 68–73 <https://doi.org/10.1016/j.clay.2017.12.001>
- [7] Esperanza Durán, Salvador Bueno, M Carmen Hermosín, Lucía Cox and Beatriz Gámiz, Optimizing a low added value bentonite as adsorbent material to remove pesticides from water, *Science of The Total Environment*, 672, (2019), 743–751 <https://doi.org/10.1016/j.scitotenv.2019.04.014>
- [8] Guillaume B Baur, Igor Yuranov and Liubov Kiwi-Minsker, Activated carbon fibers modified by metal oxide as effective structured adsorbents for acetaldehyde, *Catalysis Today*, 249, (2015), 252–258 <https://doi.org/10.1016/j.cattod.2014.11.021>
- [9] Xue Zhang, Qin Lei, Xingzhang Wang, Jianhao Liang, Chong Chen, Hong Luo, Hongmei Mou, Qiulin Deng, Tinghong Zhang and Jinlong Jiang, Removal of Cr (III) Using Humic Acid–Modified Attapulgite, *Journal of Environmental Engineering*, 145, 6, (2019), 04019028 [https://doi.org/10.1061/\(ASCE\)EE.1943-7870.0001541](https://doi.org/10.1061/(ASCE)EE.1943-7870.0001541)
- [10] Sri Sudiono, Mustika Yuniarti, Dwi Siswanta, Eko Sri Kunarti, Triyono Triyono and Sri Juari Santosa, The Role of Carboxyl and Hydroxyl Groups of Humic Acid in Removing  $AuCl_4^-$  from Aqueous Solution, *Indonesian Journal of Chemistry*, 17, 1, (2017), 95–104 <https://doi.org/10.22146/ijc.23620>
- [11] Nadezhda A Samoiloova and Maria A Krayukhina, Synthesis of magnetic chitin–adsorbent for specific proteins, *Carbohydrate polymers*, 216, (2019), 107–112 <https://doi.org/10.1016/j.carbpol.2019.03.048>
- [12] F.J. Stevenson, *Humus Chemistry: Genesis, Composition, Reactions*, 2nd ed., Wiley, 1994
- [13] Hong K. No, Samuel P. Meyers and Keun S. Lee, Isolation and characterization of chitin from crawfish shell waste, *Journal of Agricultural and Food Chemistry*, 37, 3, (1989), 575–579 <https://doi.org/10.1021/jf00087a001>
- [14] Jing-fu Liu, Zong-shan Zhao and Gui-bin Jiang, Coating  $Fe_3O_4$  Magnetic Nanoparticles with Humic Acid for High Efficient Removal of Heavy Metals in Water, *Environmental Science & Technology*, 42, 18, (2008), 6949–6954 <https://doi.org/10.1021/es800924c>
- [15] Ales Hanc, Vojtech Enev, Tereza Hrebeckova, Martina Klucakova and Miloslav Pekar, Characterization of humic acids in a continuous-feeding vermicomposting system with horse manure, *Waste Management*, 99, (2019), 1–11 <https://doi.org/10.1016/j.wasman.2019.08.032>
- [16] Ngadiwiyana Ngadiwiyana, Enny Fachriyah, Purbowatiningrum Ria Sarjono, Nor Basid Adiwibawa Prasetya, Ismiyarto Ismiyarto and Agus Subagio, Synthesis of Nano Chitosan as Carrier Material of Cinnamon's Active Component, *Jurnal Kimia Sains dan Aplikasi*, 21, 2, (2018), 92–97 <https://doi.org/10.14710/jksa.21.2.92-97>
- [17] V Enev, L Doskočil, L Kubíková and M Klučáková, The medium-term effect of natural compost on the spectroscopic properties of humic acids of Czech soils, *The Journal of Agricultural Science*, 156, 7, (2018), 877–887 <https://doi.org/10.1017/S0021859618000874>
- [18] Mohamed Traoré, Joeri Kaal and Antonio Martínez Cortizas, Application of FTIR spectroscopy to the characterization of archeological wood, *Spectrochimica Acta Part A: Molecular and Biomolecular Spectroscopy*, 153, (2016), 63–70 <https://doi.org/10.1016/j.saa.2015.07.108>
- [19] Ricka Prasdiantika, Susanto Susanto and Yustika Kusumawardani, Synthesis and Characterization of Triamine modified coated Iron Sand Hybrid Nanomaterials originating from Kendal Coast, *Jurnal Kimia Sains dan Aplikasi*, 23, 3, (2020), 68–74 <https://doi.org/10.14710/jksa.23.3.68-74>
- [20] Erzsébet Illés and Etelka Tombácz, The effect of humic acid adsorption on pH-dependent surface charging and aggregation of magnetite nanoparticles, *Journal of colloid and interface science*, 295, 1, (2006), 115–123 <https://doi.org/10.1016/j.jcis.2005.08.003>
- [21] Monireh Zarghani and Batool Akhlaghinia, Magnetically separable  $Fe_3O_4@chitin$  as an eco-friendly nanocatalyst with high efficiency for green synthesis of 5-substituted-1H-tetrazoles under solvent-free conditions, *RSC Advances*, 6, 38, (2016), 31850–31860 <https://doi.org/10.1039/C6RA07252F>
- [22] Yana Bagbi, Ankur Sarawat, Dinesh Mohan, Arvind Pandey and Pratima R. Solanki, Lead and Chromium Adsorption from Water using L-Cysteine Functionalized Magnetite ( $Fe_3O_4$ ) Nanoparticles, *Scientific Reports*, 7, 1, (2017), 7672 <https://doi.org/10.1038/s41598-017-03380-x>
- [23] Nia Siskawati, Didik Setiyo Widodo, Wasino Hadi Rahmanto and Linda Suyati, Electrosynthesis of  $\alpha-Fe_2O_3$  in a  $Fe(s)|KCl(aq)||H_2O(aq)|C(s)$  System, *Jurnal Kimia Sains dan Aplikasi*, 21, 4, (2018), 182–186 <https://doi.org/10.14710/jksa.21.4.182-186>
- [24] Philip Anggo Krisbiantoro, Sri Juari Santosa and Eko Sri Kunarti, Synthesis of Fulvic Acid-Coated Magnetite ( $Fe_3O_4$ -FA) and Its Application for the Reductive Adsorption of  $[AuCl_4]^-$ , *Indonesian Journal of Chemistry*, 17, 3, (2017), 453–460 <https://doi.org/10.22146/ijc.24828>
- [25] Erzsébet Illés and Etelka Tombácz, The role of variable surface charge and surface complexation in the adsorption of humic acid on magnetite, *Colloids and Surfaces A: Physicochemical and Engineering Aspects*, 230, 1–3, (2003), 99–109 <https://doi.org/10.1016/j.colsurfa.2003.09.017>
- [26] Soerja Koesnarpadi, Sri Juari Santosa, Dwi Siswanta and Bambang Rusdiarso, Humic Acid Coated  $Fe_3O_4$

- Nanoparticle for Phenol Sorption, *Indonesian Journal of Chemistry*, 17, 2, (2017), 274-283  
<https://doi.org/10.22146/ijc.22545>
- [27] Soerja Koesnarpadi, Sri Juari Santosa, Dwi Siswanta and Bambang Rusdiarso, Synthesis and characterization of magnetite nanoparticle coated humic acid ( $\text{Fe}_3\text{O}_4/\text{HA}$ ), *Procedia Environmental Sciences*, 30, (2015), 103-108  
<https://doi.org/10.1016/j.proenv.2015.10.018>
- [28] Liang Peng, Pufeng Qin, Ming Lei, Qingru Zeng, Huijuan Song, Jiao Yang, Jihai Shao, Bohan Liao and Jidong Gu, Modifying  $\text{Fe}_3\text{O}_4$  nanoparticles with humic acid for removal of Rhodamine B in water, *Journal of hazardous materials*, 209, (2012), 193-198  
<https://doi.org/10.1016/j.jhazmat.2012.01.011>
- [29] Hongyun Niu, Di Zhang, Shengxiao Zhang, Xiaole Zhang, Zhaofu Meng and Yaqi Cai, Humic acid coated  $\text{Fe}_3\text{O}_4$  magnetic nanoparticles as highly efficient Fenton-like catalyst for complete mineralization of sulfathiazole, *Journal of hazardous materials*, 190, 1-3, (2011), 559-565  
<https://doi.org/10.1016/j.jhazmat.2011.03.086>
- [30] Emil Zacky Effendi, Yudhi Christian Hariady, Muhammad Daffa Salaahuddin, Chairul Irawan and Iryanti Fatyasari Nata, Utilization of Rice Husk Cellulose as a Magnetic Nanoparticle Biocomposite Fiber Source for the Absorption of Manganese ( $\text{Mn}^{2+}$ ) Ions in Peat Water, *Jurnal Kimia Sains dan Aplikasi*, 22, 6, (2019), 220-226  
<https://doi.org/10.14710/jksa.22.6.220-226>
- [31] S Lagergren, Kungliga svenska vetenskapsakademiens, *Handlingar*, 24, 4, (1898), 1-39
- [32] Yuh-Shan Ho, Review of second-order models for adsorption systems, *Journal of hazardous materials*, 136, 3, (2006), 681-689  
<https://doi.org/10.1016/j.jhazmat.2005.12.043>
- [33] Zhuoxing Wang, Jiang Xu, Yunjun Hu, Heng Zhao, Junliang Zhou, Yu Liu, Zimo Lou and Xinhua Xu, Functional nanomaterials: Study on aqueous Hg (II) adsorption by magnetic  $\text{Fe}_3\text{O}_4@/\text{SiO}_2\text{-SH}$  nanoparticles, *Journal of the Taiwan Institute of Chemical Engineers*, 60, (2016), 394-402  
<https://doi.org/10.1016/j.jtice.2015.10.041>
- [34] Amina Rezgui, Eric Guibal and Taoufik Boubakera, Sorption of Hg(II) and Zn(II) ions using lignocellulosic sorbent (date pits), *The Canadian Journal of Chemical Engineering*, 95, 4, (2017), 775-782  
<https://doi.org/10.1002/cjce.22728>
- [35] Necmettin Caner, Ahmet Sarı and Mustafa Tüzen, Adsorption Characteristics of Mercury(II) Ions from Aqueous Solution onto Chitosan-Coated Diatomite, *Industrial & Engineering Chemistry Research*, 54, 30, (2015), 7524-7533  
<https://doi.org/10.1021/acs.iecr.5b01293>